

Approximate Motion Synthesis of Robotic Systems via a Polar Decomposition Based Displacement Metric

Venkatesh Venkataramanujam
 Robotics and Spatial Systems Laboratory
 Department of Mechanical and Aerospace
 Engineering
 Florida Institute of Technology
vvenkata@fit.edu

Pierre M. Larochelle
 Robotics and Spatial Systems Laboratory
 Department of Mechanical and Aerospace
 Engineering
 Florida Institute of Technology
pierrel@fit.edu

ABSTRACT

This paper presents a novel methodology for approximate motion synthesis using a PD based distance metric. Finite planar locations are represented using homogenous transformations, which can then be approximated by rotations using the polar decomposition based distance metric. A bi-invariant metric calculates the distance between two locations of a rigid body. A multidimensional nested optimization procedure is then used to determine the optimum design parameters of a planar dyad to minimize the distances from the moving dyad to a finite number of desired locations. The result is an implementation of the methodology for approximate motion synthesis.

Keywords

Kinematic synthesis, dimensional synthesis, polar decomposition, distance metrics, motion synthesis.

1. INTRODUCTION

The objective of this paper is to find the optimum design parameters for rigid body guidance through a number of desired locations¹. The synthesis procedure used here is applicable to spatial, spherical and planar motion synthesis. There exist various metrics for measuring the distance between two points in a Euclidean space. However, the notion of a metric that measures the distance between finite positions ($N > 5$) of a rigid body in plane or space that is independent of choice of coordinate system is not. The techniques used here are based on the polar decomposition (represented by PD) of the homogenous transform representation of the elements of $SE(n)$. The mapping of the elements of $SE(n-1)$ to $SO(n)$ yields hyperdimensional rotations that approximate the rigid body displacements. Figure 1 shows a representation of mapping the $z=R$ plane to elements of $SO(3)$ and figure 2 illustrates the spatial case. A bi-invariant metric may then be used to measure the distance between any two spatial or planar displacements. The result is a PD based projection on $SE(n)$ that is left invariant. These metrics find application in various areas like motion synthesis, robot calibration, motion interpolation and hybrid robot control. Other

distance metrics for spatial and planar displacements have been studied in [3, 4, 6, 7, 9, 10, 13, 14, 15, 16 and 17].

2. PD BASED PROJECTION METRIC

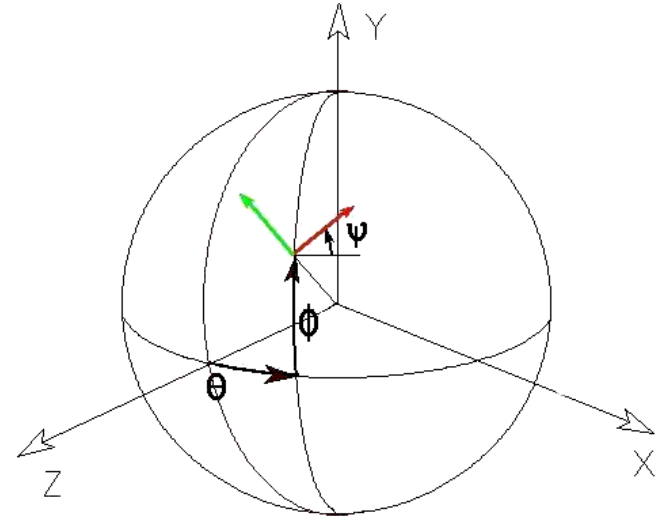


Figure 1: Planar case: $SE(2) \Rightarrow SO(3)$

The polar decomposition (PD), though perhaps less known than the singular value decomposition (SVD), is quite powerful and actually provides the foundation for the SVD. The polar decomposition of Cauchy states that “A non-singular matrix an orthogonal matrix either pre or post multiplied by a positive definite symmetric matrix”, see [18]. With respect to the our application for $T \in SE(n-1)$ its PD is $[T] = [P][Q]$, where $[P]$ and $[Q]$ are $(n \times n)$ matrices such that $[P]$ is orthogonal and $[Q]$ is positive definite and symmetric. The decomposition of $[T]$ yields $[U][diag(s_1, s_2, \dots, s_{n-1})][V]^T$ where matrices $[U]$ and $[V]$ are orthogonal and matrix $[diag(s_1, s_2, \dots, s_{n-1})]$ is positive definite and symmetric. Moreover, it is known that for full rank square matrices the polar decomposition and the singular value decomposition are related by $[P] = [U][V]^T$ and, $[Q] = [V][diag(s_1, s_2, \dots, s_{n-1})][V]^T, [11]$.

¹ Locations comprise both position and orientation

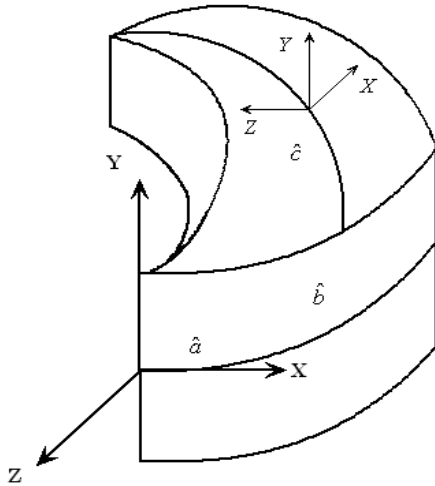
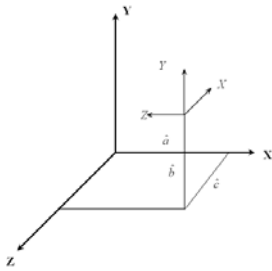


Figure 2: Spatial case: $SE(3) \Rightarrow SO(4)$

Figure 3: General case: $SE(n-1) \Rightarrow SO(n)$

Hence, for $[A] = [U][V]^T$ we have $[A] = [P]$ and conclude that the polar decomposition yields the same element of $SO(n)$. The theorem for the desired PD projection of $SE(n-1)$ onto $SO(n)$ is :

Theorem: If $T \in SE(n-1)$ and $[T] = [P][Q]$ then $[P]$ is the unique element of $SO(n)$ nearest $[T]$.

A simple and efficient iterative algorithm for the computation of the polar decomposition is shown by Dubrulle [5]. The algorithm produces mono-tonic convergence in the Frobenius norm that delivers an IEEE solution in ~ 10 or fewer steps. A *MATLAB*TM implementation of Dubrulle's Algorithm is shown in Figure 4.

```
function P = polardecomp(T)
%
%Initialization
%
P = T;
limit = (1+eps)* sqrt(size(T,2));
T = inv(P');
g = sqrt(norm(T,'fro')/norm(P,'fro'));
P = 0.5*(g*P+(1/g*T));
f = norm(P,'fro');
pf = inf;
%
% Iteration
%
while (f>limit) & (f<pf)
    pf = f;
    T = inv(P');
    g = sqrt(norm(T,'fro')/f);
    P = 0.5*(g*P+(1/g*T));
    f = norm(P,'fro');
end
return
```

Figure 4: Dubrulle's Algorithm

3. METRIC ON $SO(n)$

Given two elements $[A_1]$ and $[A_2]$ of $SO(n)$ we can define a metric using the Frobenius norm as,

$$d = || [I] - [A_2][A_1]^T ||_F \quad (1)$$

This is a valid metric as verified in [19].

4. FINITE SETS OF LOCATIONS

When a finite set of N displacements ($N \geq 2$) is given, and we wish to find the magnitude of these displacements we adopt the approach used by [12] to yield a left invariant metric. We use a unit point mass model to yield the center of mass and principal axes frame. The rationale being that the moving frame in the application areas being considered has some inherent importance. In applications such as those involving robot end effectors the moving frame is usually defined so as to coincide with the tool center point. Moreover in motion synthesis applications the moving frame is defined in such a way that its origin is at the point on the moving body whose motion is critical to the task being performed. The center of mass and the principal frame are unique to every moving body and are thus independent of the co-ordinate frame and system of units used, [12].

4.1 PRINCIPAL FRAME

The method involves determining the center of mass and the principal axes frame [PF] associated with the N prescribed locations. Each of the N locations is represented by a unit mass located at its origin:

$$\vec{c} = \frac{1}{n} \sum_{i=1}^n \vec{d}_i \quad (2)$$

Where, \vec{d}_i is the translation vector associated with the i^{th} location (i.e. the origin of the i^{th} location with respect to the fixed frame). We now proceed to define the principal axes frame [PF] which has its origin defined as the principal axes of the N point mass system with its origin at centroid \vec{c} . We may proceed by determining the inertia tensor for the N point masses;

$$[I] = \begin{bmatrix} I_{xx} & I_{xy} & I_{xz} \\ I_{yx} & I_{yy} & I_{yz} \\ I_{zx} & I_{zy} & I_{zz} \end{bmatrix} \quad (3)$$

where, the principal moments of inertia are,

$$I_{xx} = \sum_{i=1}^n (y_i^2 + z_i^2)$$

$$I_{yy} = \sum_{i=1}^n (z_i^2 + x_i^2)$$

$$I_{zz} = \sum_{i=1}^n (x_i^2 + y_i^2)$$

and, the products of inertia are,

$$I_{xy} = I_{yx} = -\sum_{i=1}^n (x_i y_i)$$

$$I_{xz} = I_{zx} = -\sum_{i=1}^n (x_i z_i)$$

$$I_{yz} = I_{zy} = -\sum_{i=1}^n (y_i z_i)$$

and, x_i , y_i and z_i are the components of the translation vector \vec{d}_i . Finally, we determine the principal frame [PF],

$$\begin{bmatrix} \vec{v}_1 & \vec{v}_2 & \vec{v}_3 & \vec{c} \\ 0 & 0 & 0 & 1 \end{bmatrix} \quad (4)$$

where, \vec{v}_i are the principal axes associated with the inertia tensor $[I]$. The direction of the vectors along the principal axes (\vec{v}_i) are chosen so that [PF] forms right-handed system.

Of importance is the fact that the principal frame does not depend on the orientations of the positions, however, the metric depends upon the orientations of the frames. Two sets of locations {A} and {B} where i^{th} locations have same origin but different orientations have the same principal frames but the distances between the members in each set are different.

4.2 Planar Case

The principal frame is determined by using the inertia tensor $[I]$. The principal axes associated with the principal frame are chosen in such a way as to form a right-handed frame. In the planar case there are 4 possible orientations of the [PF] as can be seen from Figure 5. The directions of the principal frame are chosen in such a way as to align it as closely as possible with the fixed frame. One of the ways that this may be achieved is by computing the dot product of one of the axes of the principal frame with the fixed frame.

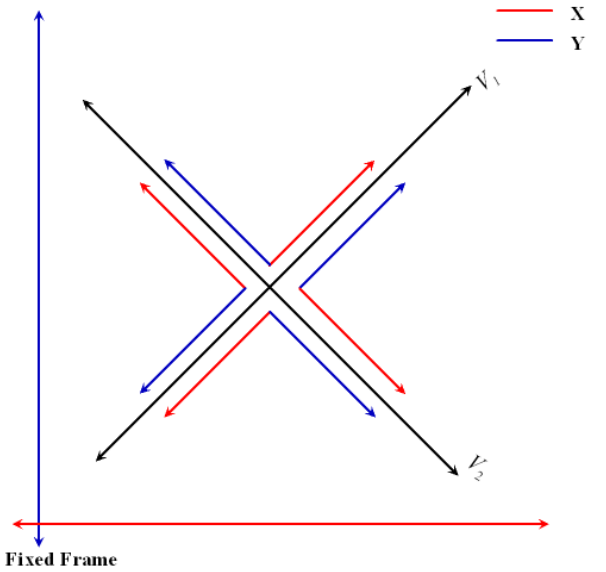


Figure 5: Four possible orientations of the principal frame.

5. CHARACTERISTIC LENGTH

The unit disparity between translation and rotation is resolved by normalizing the displacements. The displacements are normalized by choosing a characteristic length. Investigations on the use of and determination of characteristic lengths appear in see [2, 7, 13, 11, 10 and 15]. The characteristic length chosen to use, based upon the investigations reported in [7, 13], is $R = 24 \times L/\pi$, where L is the maximum translational component in the set of displacements at hand. This characteristic length is the radius of the hypersphere that approximates the translational terms by angular displacements that are $\leq 7.5(\text{deg})$. It was shown in [11] that this radius yields an effective balance between translational and rotational

displacement terms for projection metrics. The PD metric is not dependent on the choice of characteristic length. Larger characteristic length results in an increase in the weight on the rotational terms whereas if it is decreased then weight on the translational terms is increased.

6. PLANAR CASE

For determining the magnitude of the displacements we proceed as follows, [12]:

1. Determine [PF] of the N locations.
2. Determine the relative displacements from [PF] to each of the N locations.
3. Determine the characteristic length R associated with the n displacements with respect to the [PF] and scale the translation terms in each by 1/R.
4. Compute the projections of [PF] and each of the scaled relative displacements using the polar decomposition algorithm explained in 2.2.
5. The magnitude of the i^{th} displacement is defined as the distance from [PF] to the i^{th} scaled relative displacement as computed via Eq. (1). The distance between any two of the n locations is similarly computed via the application of Eq.(1) to the projected scaled relative displacements.

Since both the center of mass and principal axes are invariant with respect to the choice of co-ordinate frames as well as the system of units chosen [13, 1], the relative displacements in Step2 are left invariant.

7. CASE STUDY

Table 1: Eleven planar locations

#	X	y	α
1	-1.0000	-1.0000	90.000
2	-1.2390	-0.5529	77.362
3	-1.4204	0.3232	55.035
4	-1.1668	1.2858	30.197
5	-0.5657	1.8871	10.021
6	-0.0292	1.9547	1.712
7	0.2632	1.5598	10.030
8	0.5679	0.9339	30.197
9	1.0621	0.3645	55.035
10	1.6311	0.0632	77.362
11	2.0000	0.0000	90.000

Consider the 11 planar locations shown in Table 1, proposed by J. Michael McCarthy, U.C. Irvine for the 2002 ASME International Design Engineering Technical Conferences held in Montreal, Quebec.

The eleven planar locations are shown in Fig 6, along with the fixed reference frame [F]. We proceed to determine the centroid $\vec{C} = [0.0094 \ 0.6199]^T$. Next the principal axes are determined and the centroid and the principal axes are used to determine the [PF]. The orientation of the [PF] is chosen as suggested in 4.2.

The 11 locations are now determined with respect to the [PF]. The 11 locations with respect to the [PF] are used to determine the maximum translational component $L = 1.9493$ and $R = 24 \times 1.9493 / \pi = 14.8918$. The 11 planar locations with respect to [PF] are scaled by the characteristic length and shown in Fig 8.

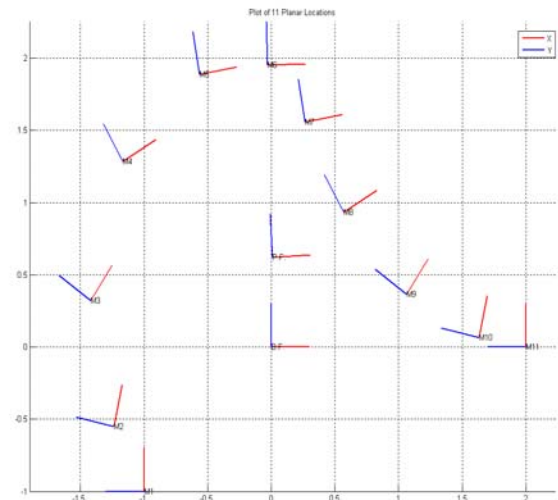


Figure 6: Locations with respect to the fixed frame

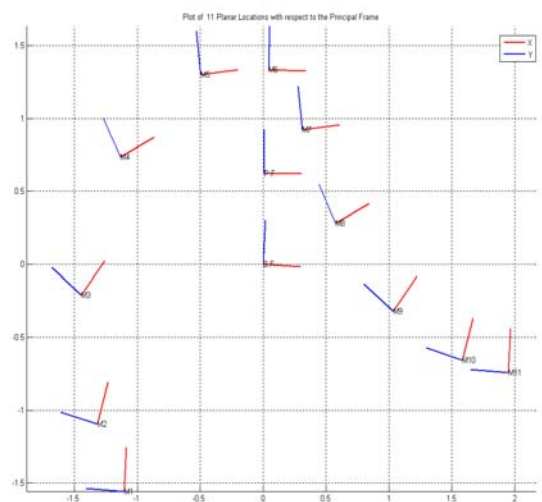


Figure 7: Locations with respect to the principal frame

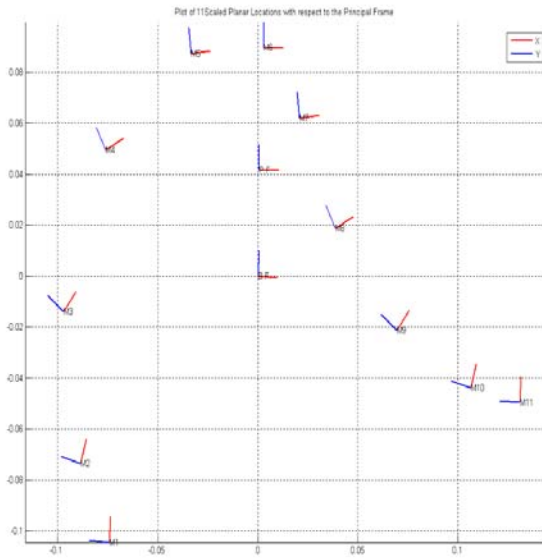


Figure 8: Scaled locations with respect to the PF

8. SYNTHESIS ALGORITHM

Given a finite set of N desired locations the task is to determine the dyad that guides the work piece through, or as near as possible, to these locations. Our approach is to utilize the metric discussed above to determine the distance from the constraint manifold to each of the n desired locations, sum these distances, and then to employ nonlinear optimization techniques to vary the dimensional synthesis parameters such that the total distance is minimized.

A planar RR dyad of length a is shown in Figure 9, the axis of the fixed joint is specified by the vector \mathbf{u} measured with respect to the fixed frame [F]. The origin of the moving frame is specified by \mathbf{v} measured in the link frame A. The dimensional synthesis variables are \mathbf{u} , \mathbf{v} and a . The homogenous transform for the forward kinematics of the dyad is given by:

$$D = x(u_x)y(u_y)z(\theta)x(a)z(\phi)x(v_x)y(v_y) \quad (5)$$

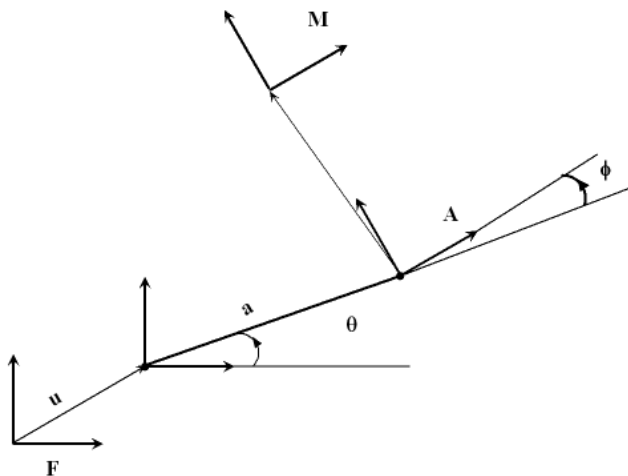


Figure 9: Planar RR dyad

Eq (5) gives us the homogenous transform of the moving frame [M] of the dyad with respect to the fixed frame. The homogenous transform is then mapped to SO(3) using the PD metric described in section 2.

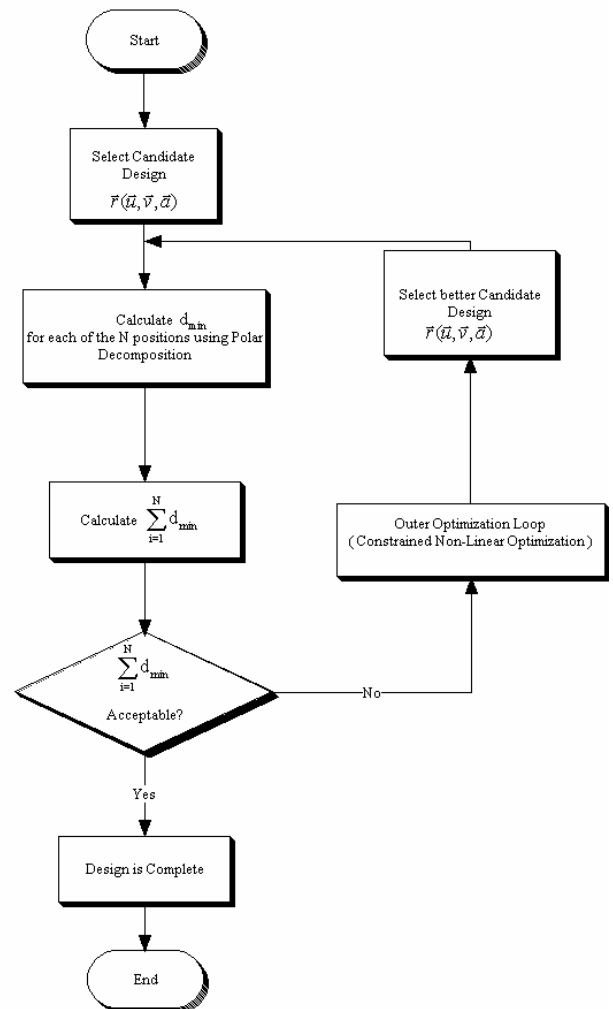


Figure 10: Outer optimization loop

The PD metric is then used to map the desired position's homogenous transform to SO(3). For each desired location the minimum distance is found by the metric described in section 3. The sum of the distances to each of the N locations is thus determined and sent to the outer optimization loop described in Fig 10, see [13].

9. CURRENT RESEARCH

The current research involves implementation of the techniques described above to synthesize planar RR dyads and closed chain mechanisms. Efforts are underway to implement the technique for planar and spatial mechanisms. Work on the implementation of GUI's using MATLAB to set up the user interface for of mechanisms is in progress. A sample of the user interface for both planar and spatial mechanisms is shown in Future design work will advance the methodology to yield a multidimensional search and optimization strategy that will

yield optimal design parameters such that the mechanisms come as close as possible to all of the N locations in a single circuit or assembly, by incorporating additional design constraints such as workspace constraints, branch, circuit and order defects.

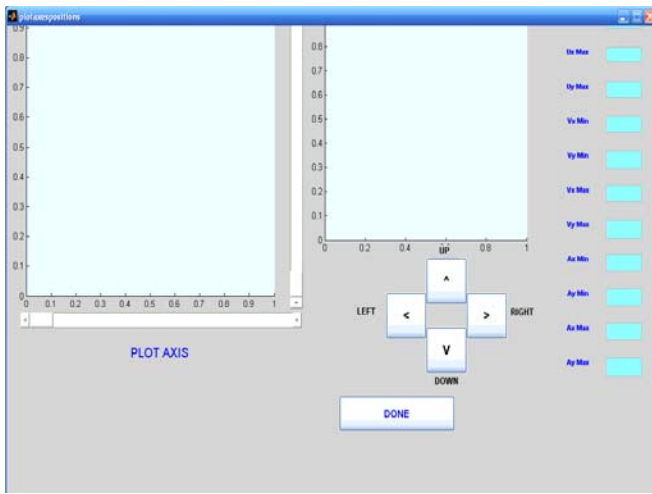


Figure 11: GUI for design of planar mechanisms

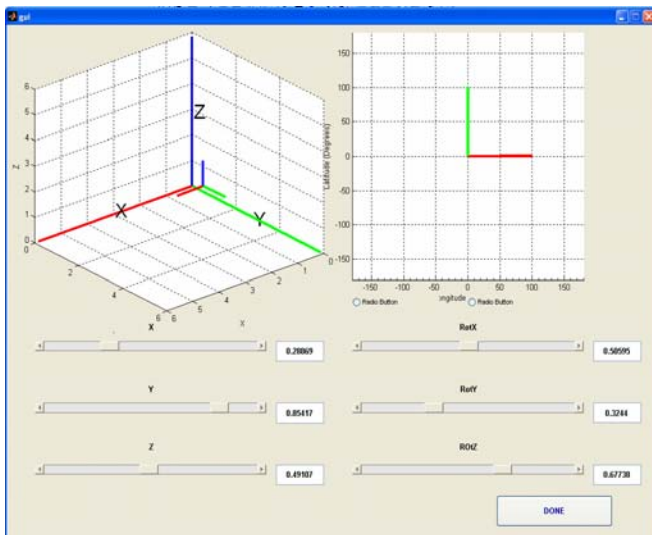


Figure 12: GUI for design of spatial mechanisms

10. ACKNOWLEDGMENTS

The material is based on research work supported by the National Science Foundation under Grant # 0422705. Any opinions, findings, and conclusions or recommendations expressed in this material are those of the author(s) and do not necessarily reflect the views of the National Science Foundation.

11. REFERENCES

- [1] Angeles, J., (2003), Fundamentals of Robotic Mechanical Systems, Springer.
- [2] Angeles, J. (2005), Is there a characteristic length of a rigid-body displacement, Proc. of the 2005 International Workshop on Computational Kinematics, Cassino, Italy.
- [3] Bobrow, J.E., and Park, F.C. (1995), On computing exact gradients for rigid body guidance using screw parameters, Proc. of the ASME Design Engineering Technical Conferences, Boston, MA, USA.
- [4] Chirikjian, G.S. (1998), Convolution metrics for rigid body motion, Proc. of the ASME Design Engineering Technical Conferences, Atlanta, USA.
- [5] Dubrulle, A.A. (2001), An optimum iteration for the matrix polar decomposition, Electronic Transaction on Numerical Analysis, vol.8, pp. 21-25.
- [6] Eberharter, J., and Ravani, B., (2004), Local metrics for rigid body displacements, ASME Journal of Mechanical Design, vol. 126, pp.805-812.
- [7] Etzel, K., and McCarthy, J.M. (1996), A metric for spatial displacements using biquaternions on $SO(4)$, Proc. of the IEEE International Conference on Robotics and Automation, Minneapolis, USA.
- [8] Greenwood, D.T., (2003), Advanced Dynamics, Cambridge University Press.
- [9] Gupta, K.C. (1997), Measures of positional error for a rigid body, ASME Journal of Mechanical Design, vol. 119, pp. 346-349.
- [10] Kazerounian, K., and Rastegar, J., (1992), Object norms: A class of coordinate and metric independent norms for displacements, Proc. of the ASME Design Engineering Technical Conferences, Scottsdale, USA.
- [11] Larochele, P. (1999), On the geometry of approximate bi-invariant projective displacement metrics, Proc. of the World Congress on the Theory of Machines and Mechanisms, Oulu, Finland.
- [12] Larochele, P., "A Polar Decomposition Based Displacement Metric for a Finite Region of $SE(n)$ ", Proceedings of the 10th International Symposium on Advances in Robot Kinematics (ARK), Lubljana, Slovenia, June 25-29, 2006.
- [13] Larochele, P., and McCarthy, J.M. (1995), Planar motion synthesis using an approximate bi-invariant metric, ASME Journal of Mechanical Design, vol. 117, no. 4, pp. 646-651.
- [14] Lin, Q., and Burdick, J. (2000), Objective and Frame-Invariant Kinematic Metric Functions for rigid bodies, International Journal of Robotics Research, vol. 19, n. 6, pp. 612-625.
- [15] Martinez, J.M.R., and Duffy, J. (1995), On the metrics of rigid body displacements for infinite and finite bodies, ASME Journal of Mechanical Design, vol. 117, pp. 41-47.
- [16] Park, F.C., (1995), Distance metrics on the rigid-body motions with applications to mechanism design, ASME Journal of Mechanical Design, vol. 117, no. 1, pp. 48-54.
- [17] Tse, D.M., Larochele, P.M. (2000), Approximating spatial locations with spherical orientations for spherical mechanism design, ASME Journal of Mechanical Design, vol. 122, pp. 457-463.
- [18] Halmos, P.R., (1990), Finite Dimensional Vector Spaces, Van Nostrand.
- [19] Schilling, R.J., and Lee, H., (1988), Engineering Analysis-a Vector Space Approach, Wiley & Sons.